

CuFe₂O₄ as a heterogeneous Fenton catalyst for the removal of ciprofloxacin from aqueous solution at natural pH

Nurul Najwa Mohamad Jani^a, Saifullahi Shehu Imam^{b*}, Alamri Rahmah Dhahawi Ahmad^a, Rohana Adnan^{a*}

^aSchool of Chemical Sciences, Universiti Sains Malaysia, 11800, Penang, Malaysia

^bDepartment of Pure and Industrial Chemistry, Bayero University P.M.B 3011, Kano, Nigeria

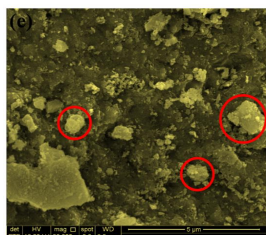
*Corresponding Author: r_adnan@usm.my; ssimam.chm@buk.edu.ng

Article history :

Received 29 September 2021

Accepted 14 November 2021

GRAPHICAL ABSTRACT



ABSTRACT

In the present study, a bimetallic oxide catalyst of CuFe₂O₄ was synthesized via facile co-precipitation process and characterized using various techniques such as X-ray diffraction (XRD), Fourier transform infrared spectroscopy (FTIR), field emission scanning electron microscope (FESEM), energy dispersive X-ray (EDX), N₂ adsorption – desorption analysis and UV-visible spectroscopy. Subsequently, it was used to degrade ciprofloxacin (CIP), a fluoroquinolone antibiotic, from an aqueous solution via the Fenton process under various conditions. The effect of several operational parameters such as catalyst dosage, H₂O₂ volume, initial CIP concentration, inorganic ions, and solar irradiation has also been evaluated. The removal process was found to follow the trend: photo-Fenton > Fenton > catalytic > adsorption > photolysis. The results showed that the CuFe₂O₄ catalyst degraded a high percentage of CIP and maintained reasonable efficiency even after five cycles, thus indicating that CuFe₂O₄ is a promising catalyst for the activation of H₂O₂ to degrade antibiotics.

Keywords: CuFe₂O₄; Heterogeneous catalyst; Fenton oxidation; Ciprofloxacin; Wastewater treatment.

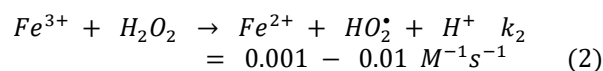
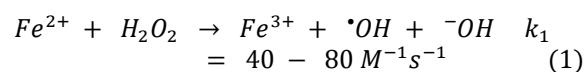
© 2021 School of Chemical and Engineering, UTM. All rights reserved
| eISSN 0128-2581 |

1. INTRODUCTION

Ciprofloxacin (CIP) is a second-generation quinolone antibiotic widely used for medical treatments due to its strong antibacterial activity [1]. However, CIP is only partially metabolized by the body after ingestion, and around 20% - 80% of the drug is excreted back in pharmacologically active form into the water bodies [2-4]. Its presence in water has been reported to inhibit the growth of spinach plants, affect non-intended pathogens, lead to the development of antibiotic-resistant bacteria, and the risk of consuming water contaminated by CIP [5-7]. Unfortunately, studies have shown that traditional wastewater treatment techniques do not remove low CIP concentrations [8]. Thus, it is critically essential to exploit more effective methods for the removal of CIP.

Fenton process is one of the most famous advanced oxidation processes (AOPs), which has attracted significant attention due to its low toxicity, high efficiency, and simple operation [9]. The process initially involves the generation of reactive oxygen species (specifically hydroxyl radicals ([•]OH)) via catalytic decomposition of H₂O₂ by Fe²⁺ (Eq. 1). Subsequently, regeneration of Fe²⁺ is possible via the

reduction of Fe³⁺ using H₂O₂ (Eq. 2) [10]. Nowadays, researchers have focused more on heterogeneous Fenton catalysis due to the ease of recovery of the catalyst [11].



CuFe₂O₄ is a spinel ferrite with high catalytic performance and is catalytically more stable than CuFeO₂ [12, 13]. It is commonly used as a catalyst in hydrogen production from oxygenated hydrocarbons [14], decomposition of gaseous pollutants [15], water gas shift reaction [16], and in activating oxidizing agents [17]. In the current study, CuFe₂O₄ would be prepared via a facile co-precipitation process and characterized using various techniques. Subsequently, the catalytic ability and stability of CuFe₂O₄ would also be evaluated by removing CIP antibiotics from an aqueous solution.

2.0 MATERIALS AND METHODS

2.1 Chemicals

All chemicals were analytical grade and were used without further purification. Copper (II) nitrate trihydrate ($\text{Cu}(\text{NO}_3)_2 \cdot 3\text{H}_2\text{O}$), iron (III) nitrate nonahydrate ($\text{Fe}(\text{NO}_3)_3 \cdot 9\text{H}_2\text{O}$), sodium hydroxide (NaOH), hydrogen peroxide (H_2O_2 , 30%), sodium nitrate (NaNO_3) and sodium bicarbonate (NaHCO_3) were supplied by QReC (Asia). Sodium sulphate anhydrous (Na_2SO_4) and sodium chloride (NaCl) were from Bendosen Laboratory Chemicals. Ciprofloxacin ($\text{C}_{17}\text{H}_{18}\text{FN}_3\text{O}_3$) was obtained from Fluka Chemicals. Distilled water was used during the preparation of all solutions.

2.2 Synthesis of CuFe_2O_4

CuFe_2O_4 was prepared using the method reported by Hegazy *et al.* [18] with slight modifications. As much as 0.025 moles of copper nitrate ($\text{Cu}(\text{NO}_3)_2 \cdot 3\text{H}_2\text{O}$) and 0.05 mole of iron nitrate ($\text{Fe}(\text{NO}_3)_3 \cdot 9\text{H}_2\text{O}$) were dissolved together in a beaker containing 100 mL of distilled water under continuous stirring at room temperature. The precipitation reaction was performed by adding 75 mL of 4 M sodium hydroxide solution dropwise into the above mixture with moderate stirring and reaction temperature maintained at 90 °C for 3 hours. The resulting product was filtered and washed several times with distilled water until a constant pH of ~8 was attained. The product was then dried at 60 °C in an oven overnight. Subsequently, the dried product was grounded, and calcination was performed at 400 °C for 4 hours with a heating rate of 10 °C/min under an air atmosphere. The resulting product was blackish CuFe_2O_4 powder.

2.3 Characterization

The crystal structure of CuFe_2O_4 was characterized using X-ray powder diffractometer (BRUKER D8) with $\text{Cu-K}\alpha$ radiation over 2θ scanning range of 10 – 90°. Surface morphology and elemental composition were investigated using Carl Zeiss Leo Supra field emission scanning electron microscope (FESEM) with Oxford instrument X-max Energy dispersive X-ray (EDX). UV-vis analysis was conducted using Perkin Elmer Lambda 35 spectrometer equipped with diffuse reflectance attachment. FTIR spectra was measured using Perkin Elmer 2000 in the wavenumber range of 400 – 3600 cm^{-1} . The specific surface area of CuFe_2O_4 was determined using Micromeritics ASAP 2020 V 4.01 at liquid nitrogen temperature (-196 °C).

2.4 Removal study

All experiments were conducted using a constant working liquid volume of 100 mL in 250 mL glass beakers. The effect of catalyst dosage was conducted by using various amounts of CuFe_2O_4 (0.25, 0.50, 0.75, 1.0, 1.25 and 1.50 g/L) and 0.5 mL 30% H_2O_2 for degrading 20 mg/L of CIP.

To investigate the effect of volume of H_2O_2 , experiments were carried out by adding either 0.3, 0.5, or 0.7 mL of 30% H_2O_2 to 20 mg/L CIP solution with 1.0 g/L catalyst dosage. The effect of initial CIP concentration was studied by adding 1.0 g/L of CuFe_2O_4 and 0.5 mL of 30% H_2O_2 to 100 mL of 5, 10, 15, 20, 30, and 40 mg/L of CIP solutions. Since organic pollutants and inorganic ions often coexist in real wastewater, the effect of inorganic ions on the degradation of 20 mg/L aqueous CIP solution using 0.5 mL of 30% H_2O_2 was carried out by adding 10 mM of either NaCl , NaNO_3 , NaHCO_3 , or Na_2SO_4 salts. The effect of solar irradiation on the Fenton/catalytic degradation of 20 mg/L aqueous CIP solution was also studied by carrying out reactions under optimized conditions at Penang, Malaysia between 12:00 – 2:00 pm in February 2020. Finally, the used catalyst was recovered for the reusability studies, washed several times with distilled water and ethanol, and dried at 60 °C overnight in an oven. All experiments were conducted at the natural pH of the aqueous CIP solution, which was 7.10 ± 0.1 .

CIP degradation was measured spectroscopically using a Shimadzu UV-2600 UV-Vis spectrometer by withdrawing 5 mL of the reaction suspension, centrifuged immediately at 3500 rpm for 5 min, and the absorbance of remnant CIP was measured at $\lambda_{\text{max}} = 276$ nm. The percentage of catalytic degradation of CIP was calculated using Eq. 3:

$$\begin{aligned} \% \text{ CIP removal} \\ &= \frac{A_o - A}{A_o} \end{aligned} \quad (3)$$

where A_o is the initial CIP absorbance before degradation and A is the CIP absorbance after degradation.

3.0 RESULTS AND DISCUSSION

3.1 Characterization of CuFe_2O_4 catalyst

Fig. 1(a) shows the XRD pattern of the CuFe_2O_4 catalyst. The diffraction peaks at $2\theta = 35.5^\circ$, 36.9° , 43.2° , 57.8° and 62.2° corresponds to the (311), (222), (400), (511) and (440) planes of cubic CuFe_2O_4 (JCPDS NO: 25-0283) respectively [19, 20]. The wide peak at about $2\theta = 23^\circ$ is an indication that the crystalline structure of CuFe_2O_4 combined or interfered over amorphous surroundings [21]. The FTIR spectrum of CuFe_2O_4 in the range of 400 – 3600 cm^{-1} is presented in Fig. 1(b). In general, spinel ferrites have two metal-oxygen bands in their spectra. The lower frequency band is usually located within the 450 – 385 cm^{-1} region, while the higher frequency band is found within the 600 – 550 cm^{-1} region [22]. In the case of the CuFe_2O_4 catalyst, the peak at about 590 and 440 cm^{-1} are attributed to Fe – O and Cu – O bonds [23]. The band at about 3400 cm^{-1} is due to the hydroxyl functional group, while the peak at 1600 cm^{-1} is due to the bending vibration of adsorbed water molecules [24, 25]. Such results from FTIR have further confirmed the successful CuFe_2O_4 synthesis. Fig. 1(c) is the

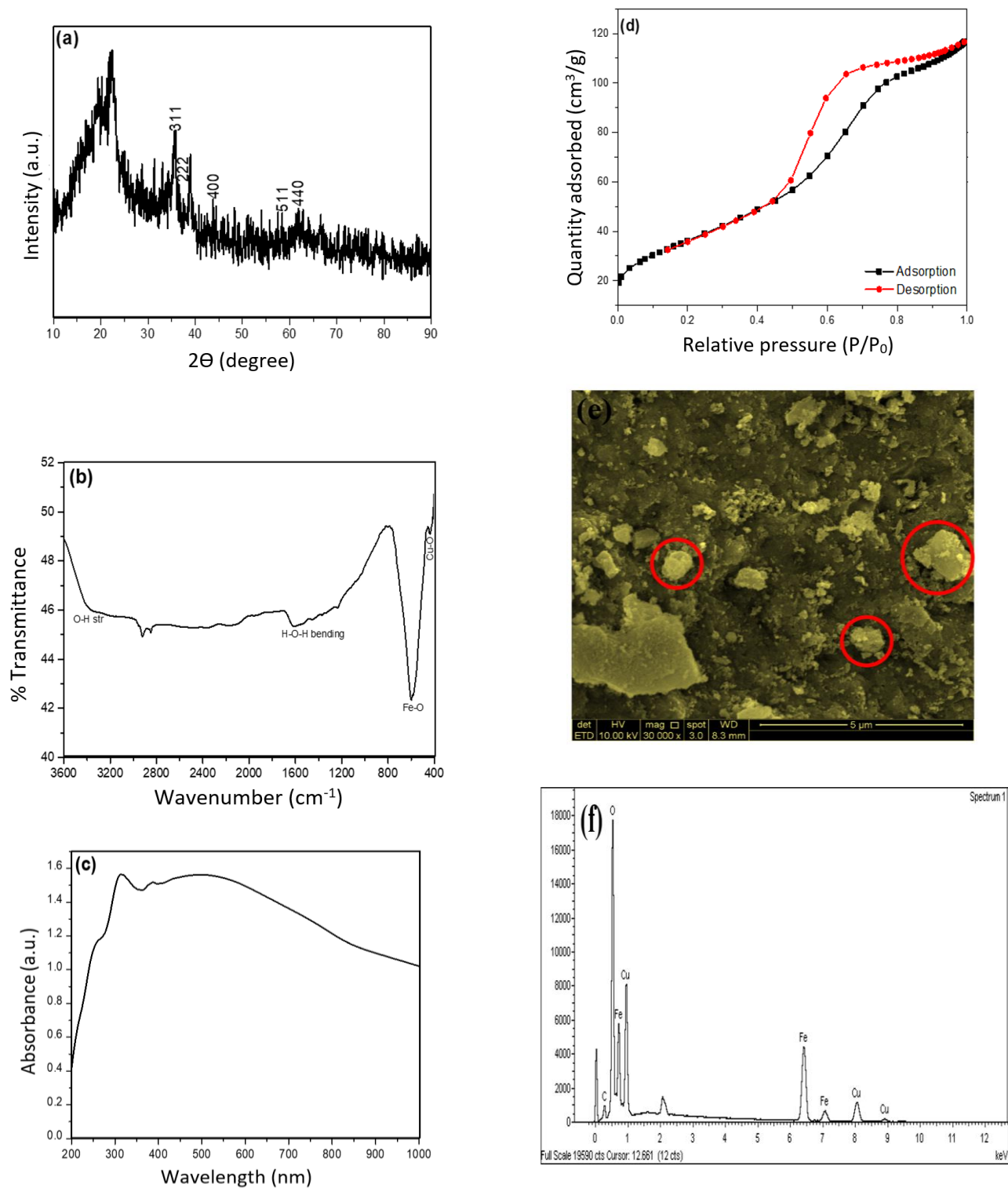


Fig. 1. (a) XRD pattern (b) FTIR spectrum (c) UV-Vis spectrum, (d) N_2 adsorption-desorption isotherm, (e) FESEM image and (f) EDX of CuFe_2O_4

absorption spectra of CuFe_2O_4 , and the absorption band between 310 – 340 nm is assigned to the CuFe_2O_4 characteristic bond [26]. In the current study, a band is observed at about 320 nm and is close to the value reported for CuFe_2O_4 by Hammad *et al.* [27].

N_2 adsorption-desorption isotherm curve of CuFe_2O_4 is shown in Fig. 1(d). Based on the results, the CuFe_2O_4 catalyst exhibits a type IV isotherm with H1 hysteresis loop which is attributed to rigid, well-defined, and unconnected pores [28]. The BET surface area of CuFe_2O_4 was determined as 120.15 m^2/g . Fig. 1(e) shows the morphology of CuFe_2O_4 catalyst consists of irregular and agglomerated particles (some of which have been cycled). The EDX spectra presented in Fig. 1(f) confirm the presence of Cu, Fe, and O in CuFe_2O_4 . The carbon signal could be due to the adventitious carbon from the atmosphere or the conductive tape used during analysis [29].

3.2 CIP removal process

The effect of various operational parameters such as catalyst dosage, H_2O_2 volume, initial CIP concentration, inorganic ions, and solar irradiation on CIP removal from aqueous solution via heterogeneous catalysis using CuFe_2O_4 have been examined and the findings are discussed in the subsequent sections.

3.2.1 Effect of catalyst dosage

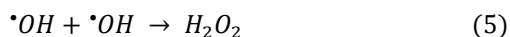
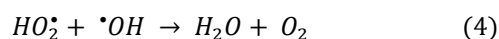
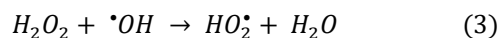
The effect of catalyst dosage on CIP removal from aqueous solution via adsorption and heterogeneous Fenton degradation was studied using 0.25 – 1.5 g/L of CuFe_2O_4 . The results are shown in Fig. 2(a-b). Based on Fig. 2a, the adsorption of CIP using CuFe_2O_4 increases with an increase in catalyst dosage. The percentages of CIP removed after 120 min using 0.25, 0.5, 0.75, 1.0, 1.25 and 1.5 g/L of CuFe_2O_4 catalyst were 9, 23, 29, 37, 41 and 46%. Such performance is attributed to the increase in active sites and catalyst dosage [30]. Moreover, as the removal percentage remain unchanged after 100 min, it was taken as the equilibrium time for CIP adsorption using different dosages of CuFe_2O_4 .

In the case of heterogeneous Fenton degradation of CIP in the presence of H_2O_2 using CuFe_2O_4 catalyst presented in Fig. 2b, the percentage removal was also found to increase with an increase in catalyst dosage. The percentages removal after 120 min using 0.25, 0.5, 0.75, 1.0, 1.25 and 1.5 g/L of CuFe_2O_4 catalyst were 29, 55, 64, 75, 79 and 80%. Such performance could be attributed to the increase in the number of active sites on the catalyst surface, which was projected to accelerate and enhance the hydroxyl radical production by the reactions of hydrogen peroxide decomposition [31]. However, only a slight increase in removal percentage was observed by increasing the catalyst dosage from 1.25 – 1.5 g/L. This could probably be due to the inhibition effect when iron species exist in excess, in

which they behaved as scavengers of hydroxyl radicals [32]. Based on the results obtained, the optimum CuFe_2O_4 catalyst dosage of 1.0 g/L was used for the rest of the study.

3.2.2 Effect of H_2O_2 volume

The optimization for H_2O_2 was carried out by varying the volumes of H_2O_2 from 0.3 to 0.7 mL, and the results are shown in Fig. 2c. Based on the results obtained, compared to the percentage of CIP removal recorded using 0.3 and 0.7 mL of H_2O_2 , the percentage of removal using 0.5 mL of H_2O_2 is higher. From the figure, increasing the H_2O_2 volume from 0.3 to 0.5 mL generally had a positive effect on CIP removal because theoretically, the higher H_2O_2 volume will generate more hydroxyl radical. However, this was not always the case. For instance, the degradation of CIP decreases from 70 to 56% when the volume of H_2O_2 is increased from 0.5 to 0.7 mL. This could be explained by a critical concentration of H_2O_2 in the Fenton process. As the concentration of H_2O_2 increases beyond the critical value, it becomes a hydroxyl radical ($\bullet\text{OH}$) scavenger, but the effect is more pronounced at a shorter reaction time, as reported in a previous study [33, 34]. Excess H_2O_2 will also react with $\bullet\text{OH}$ to form hydroperoxyl radical ($\text{HO}_2\bullet$), with a lower reduction potential value than $\bullet\text{OH}$ [35]. The $\text{HO}_2\bullet$ can scavenge $\bullet\text{OH}$ to form water and oxygen, as shown in Eq. 4 [32]. The recombination of $\bullet\text{OH}$ shown in Eq. 5 could also affect the percentage removal if excess H_2O_2 is present [36].



3.2.3 Effect of initial CIP concentration

The study of the dependence of percentage of removal on the initial concentration of the CIP is significant from an application point of view. For this purpose, the dependence of CIP adsorption and degradation on CIP initial concentration has been investigated over the range of 5 to 40 mg/L with an optimum H_2O_2 volume of 0.5 mL. As shown in Fig. 2d, the percentage of removal via adsorption decreases from about 32 to 23% when the concentration of CIP was increased from 10 to 40 mg/L. Such effect is attributed to the high competition for active sites with the increase in initial CIP concentration [37]. In the case of the Fenton degradation process, the percentage of CIP removal using 5 to 30 mg/L does not show much difference and stays around 78-80%. However, when the concentration is 40 mg/L, the removal percentage drops to 70%. The apparent reason for this is that when the initial concentration of the CIP increases, the hydroxyl radical concentrations for all CIP remain constant since the volume of H_2O_2 was fixed at 0.5 mL. Another contributing factor is that at high CIP

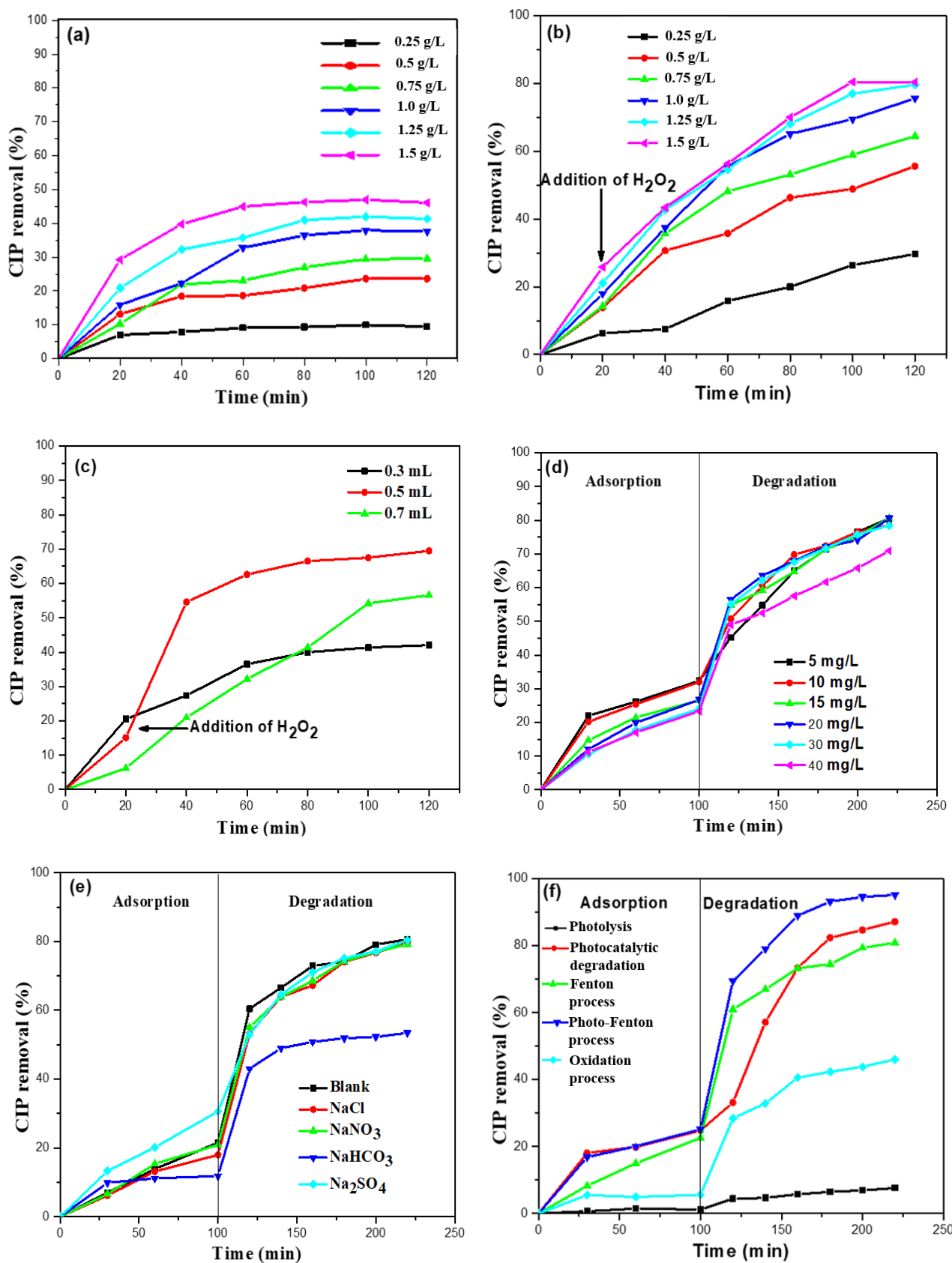


Fig. 2. Effect of some operational parameters on the removal of CIP (a-b) catalyst dosage with and without H₂O₂, (c) volume of H₂O₂, (d) initial CIP concentration, (e) inorganic ions, and (f) solar irradiation.

concentration, the number of active sites available on CuFe_2O_4 for hydroxyl radical production by the reactions of hydrogen peroxide decomposition also decreases due to the competitive adsorption of CIP molecules on its surface [38]. The concentration of CIP was set at 20 mg/L to reflect the higher end concentration for antibiotics found in wastewater and treated wastewater [39] and based on the results, it is expected that the catalysts will be efficient to treat CIP at concentrations lower than 20 mg/L.

3.2.4 Effect of inorganic ions

The effect of various inorganic ions such as Cl^- , NO_3^- , HCO_3^- and SO_4^{2-} on the removal of CIP have also been studied, and the results are shown in Fig. 2e. In the presence of Cl^- , NO_3^- and SO_4^{2-} , no significant decrease in degradation efficiency was observed. However, in the presence of HCO_3^- , the percentage removal decreased from 80.6 to 53.4%. This is because HCO_3^- is a hydroxyl radical scavenger which inhibit the degradation of CIP [40].

3.2.5 Effect of solar irradiation

The degradation of CIP in aqueous solution by various processes i.e. photolysis (A), photocatalytic degradation (B), Fenton process (C), photo-Fenton process (D) and oxidation process (E) have been studied, and the results are shown in Fig. 2f. The removal of CIP from aqueous solution via photocatalytic degradation, photo-Fenton, and oxidation processes involves exposure to solar irradiation. The results showed that upon exposure of aqueous CIP solution to solar irradiation but in the absence of CuFe_2O_4 or H_2O_2 , a very small reduction in CIP concentration (7%) was observed. However, in the presence of CuFe_2O_4 i.e. process B, as much as 87% removal was achieved. This showed that CuFe_2O_4 has excellent photocatalytic ability to eliminate CIP under solar irradiation. Meanwhile, the degradation of CIP via the photo-Fenton process (D) is more effective than the Fenton process (C). Up to 95% removal was achieved via the former process compared to only 80% degradation efficiency recorded using the Fenton process (C). It could be possible that the formation of hydroxyl radicals is higher under light exposure (photo-Fenton process) thus leading to a relatively higher degradation efficiency compared to the Fenton process.

3.3 Reusability and stability of CuFe_2O_4

The reusability and stability of a catalyst are essential for practical application. For this purpose, the recycling efficiency of CuFe_2O_4 for the removal of CIP was studied in five cycles consecutively. Based on the result presented in Fig. 3a, the percentage of CIP removal using CuFe_2O_4 dropped to 49% after the fifth cycle. Previously,

Wang and co-workers also observed a decrease in the percentage of norfloxacin removal using CuFe_2O_4 as an activator of peroxymonosulfate, from 91.8 to 78.3% after four cycles [41]. They attributed such a decrease in the percentage of removal to the conglomeration of the catalyst and occupation of the active sites of CuFe_2O_4 by norfloxacin or its intermediates [41]. However, the FTIR spectra of CuFe_2O_4 catalyst before use and after the fifth cycle presented in Fig. 3b did not show any significant change in the functional groups, indicating that the CuFe_2O_4 behaves as a catalyst and is structurally stable.

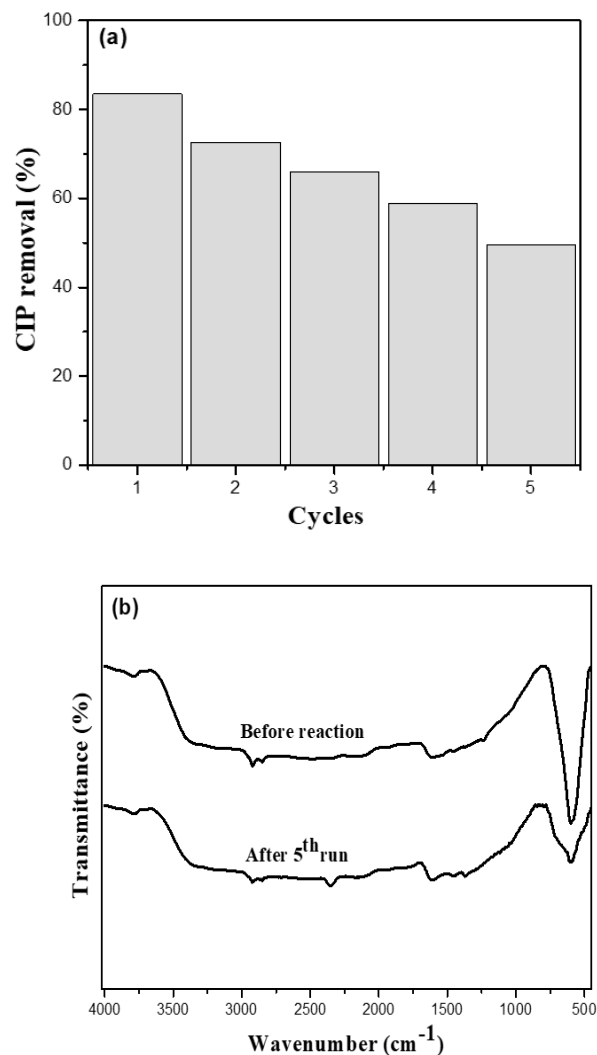


Fig. 3. (a) Reusability of CuFe_2O_4 catalyst in the removal of CIP from aqueous solution via Fenton reaction (b) FTIR spectra of fresh and used CuFe_2O_4 catalyst after the fifth cycle.

4. CONCLUSION

In the current study, CuFe_2O_4 catalyst was successfully synthesized via facile co-precipitation process and

characterized using various techniques. Subsequently, CuFe_2O_4 catalyst was used as an activator of H_2O_2 for the degradation of CIP from an aqueous solution. The degradation process was affected by several parameters such as catalyst dosage, the volume of H_2O_2 , initial CIP concentration, inorganic ions, and solar irradiation. The optimal conditions for the removal of CIP from an aqueous solution using the CuFe_2O_4 catalyst are 1.0 g/L catalyst dosage, 0.5 mL of H_2O_2 and 2 h exposure under sun light. The highest removal percentage of more than 90% was recorded via the heterogeneous photo-Fenton degradation process under solar irradiation. The reusability study shows that the catalyst maintained reasonable efficiency, although a slight reduction was observed after the fifth cycle although the FTIR analysis revealed no changes in the surface functional group. Although further study should be done to improve the reusability of the CuFe_2O_4 catalyst, the current study revealed that it could be a good candidate for the treatment of wastewater contaminated by organic pollutants.

ACKNOWLEDGEMENTS

The authors gratefully thank Universiti Sains Malaysia for the financial support provided under RUI Grant No. 1001/PKIMIA/8011117.

REFERENCES

- [1] X. Hou, J. Liu, W. Guo, S. Li, Y. Guo, Y. Shi, C. Zhang, *Catalysis Communications* 121 (2019) 27-31.
- [2] N. Lu, P. Wang, Y. Su, H. Yu, N. Liu, X. Quan, *Chemosphere* 215 (2019) 444-453.
- [3] S.S. Imam, R. Adnan, N.H.M. Kaus, *Journal of Alloys and Compounds* (2020) 155990.
- [4] M.A.M. Yusoff, S.S. Imam, I. Shah, R. Adnan, *Materials Research Express* 6(8) (2019) 0850g5.
- [5] S.S. Imam, R. Adnan, N.H.M. Kaus, *SN Applied Sciences* 1(8) (2019) 845.
- [6] M. Malakootian, A. Nasiri, A. Asadipour, E. Kargar, *Process Safety and Environmental Protection* 129 (2019) 138-151.
- [7] S.S. Imam, R. Adnan, N.H.M. Kaus, *Colloids and Surfaces A: Physicochemical and Engineering Aspects* 585 (2020) 124069.
- [8] Y. Huang, L.-c. Nengzi, X. Zhang, J. Gou, Y. Gao, G. Zhu, Q. Cheng, X. Cheng, *Chemical Engineering Journal* 388 (2020) 124274.
- [9] Y. Xiang, Y. Huang, B. Xiao, X. Wu, G. Zhang, *Applied Surface Science* 513 (2020) 145820.
- [10] J. da Silveira Salla, K. da Boit Martinello, G.L. Dotto, E. García-Díaz, H. Javed, P.J. Alvarez, E.L. Foletto, *Colloids and Surfaces A: Physicochemical and Engineering Aspects* (2020) 124679.
- [11] Y. Pang, H. Lei, *Chemical Engineering Journal* 287 (2016) 585-592.
- [12] J. Wu, X. Wang, H. Kang, J. Zhang, C. Yang, *International journal of environmental studies* 71(4) (2014) 534-545.
- [13] Z. Chen, L. Wang, H. Xu, Q. Wen, *Chemical Engineering Journal* 389 (2020) 124345.
- [14] K. Faungnawakij, N. Shimoda, T. Fukunaga, R. Kikuchi, K. Eguchi, *Applied Catalysis B: Environmental* 92(3-4) (2009) 341-350.
- [15] W. Shangguan, Y. Teraoka, S. Kagawa, *Applied Catalysis B: Environmental* 16(2) (1998) 149-154.
- [16] M. Estrella, L. Barrio, G. Zhou, X. Wang, Q. Wang, W. Wen, J.C. Hanson, A.I. Frenkel, J.A. Rodriguez, *The Journal of Physical Chemistry C* 113(32) (2009) 14411-14417.
- [17] D. Karimipourfard, R. Eslamloueyan, N. Mehranbod, *Journal of Environmental Chemical Engineering* 8(2) (2020) 103426.
- [18] E.Z. Hegazy, I.H. Abd El-Maksod, A.M. Ibrahim, S.E.-S. El-Shafay, *Bulletin of the National Research Centre* 42(1) (2018) 9.
- [19] X. Wu, F. Xia, Z. Nan, *Materials Chemistry and Physics* 242 (2020) 122490.
- [20] R. Dhanda, M. Kidwai, *RSC advances* 6(58) (2016) 53430-53437.
- [21] A.M. Naglah, M.A. Al-Omar, A.A. Almehezia, H.M. AlKahtani, A.J. Obaidullah, M.A. Bhat, N.S. Al-Shakliah, *Journal of Inorganic and Organometallic Polymers and Materials* 31(5) (2021) 2105-2115.
- [22] K.C. Das, S.S. Dhar, *Journal of Alloys and Compounds* (2020) 154462.
- [23] F. Foroughi, S. Hassanzadeh-Tabrizi, A. Bigham, *Materials Science and Engineering: C* 68 (2016) 774-779.
- [24] G. Mathubala, A. Manikandan, S.A. Antony, P. Ramar, *Journal of Molecular Structure* 1113 (2016) 79-87.
- [25] S.T. Fardood, F. Moradnia, M. Mostafaei, Z. Afshari, V. Faramarzi, S. Ganjkanlu, *Nanochem. Res.* 4 (2019) 86-93.
- [26] U. Naresh, R.J. Kumar, T.R. Parasad, *Bulletin of Pure & Applied Sciences-Physics* 37(2) (2018) 172-177.
- [27] T.M. Hammad, J.K. Salem, A.A. Amsha, N.K. Hejazy, *Journal of Alloys and Compounds* 741 (2018) 123-130.
- [28] E. Barsotti, S.P. Tan, M. Piri, J.-H. Chen, *Fuel* 263 (2020) 116441.
- [29] S.S. Imam, R. Adnan, N.H.M. Kaus, *Research on Chemical Intermediates* 44(9) (2018) 5357-5376.
- [30] I. Shah, R. Adnan, W.S.W. Ngah, N. Mohamed, *PLoS one* 10(4) (2015) e0122603.
- [31] E.M. Cuerda-Correa, M.F. Alexandre-Franco, C. Fernández-González, *Water* 12(1) (2020) 102.
- [32] M.E. Ali, T.A. Gad-Allah, M.I. Badawy, *Applied Water Science* 3(1) (2013) 263-270.
- [33] M.Y. Ghaly, G. Härtel, R. Mayer, R. Haseneder, *waste management* 21(1) (2001) 41-47.
- [34] N. Azmi, O. Ayodele, V. Vadivelu, M. Asif, B. Hameed, *Journal of the Taiwan Institute of Chemical Engineers* 45(4) (2014) 1459-1467.
- [35] Y. Deng, R. Zhao, *Current Pollution Reports* 1(3) (2015) 167-176.
- [36] C. Bouasla, F. Ismail, M.E.-H. Samar, *International Journal of Industrial Chemistry* 3(1) (2012) 15.
- [37] N. Singh, C. Balomajumder, *Journal of water process engineering* 9 (2016) 233-245.
- [38] H. Hassan, B. Hameed, *Chemical Engineering Journal* 171(3) (2011) 912-918.
- [39] J. Fick, H. Söderström, R.H. Lindberg, C. Phan, M. Tysklind, D.J. Larsson, *Environmental Toxicology and Chemistry* 28(12) (2009) 2522-2527.
- [40] Y. Kanigaridou, A. Petala, Z. Frontistis, M. Antonopoulou, M. Solakidou, I. Konstantinou, Y. Deligiannakis, D. Mantzavinos, D.I. Kondarides, *Chemical Engineering Journal* 318 (2017) 39-49.
- [41] Y. Wang, D. Tian, W. Chu, M. Li, X. Lu, *Separation and Purification Technology* 212 (2019) 536-544.